



Numerical Study of the Influence of the Excitons Level in Semiconductors Supply of a Network VPLS IP/MPLS

Modou Faye¹, Cheikh Mbow², Ibrahima Wade³, Modou Pilor⁴, Bassirou Ba⁵
^{1,2,3,4,5} Department of Physics, Faculty of Science, University Cheikh Anta Diop, Dakar, Senegal
(¹fayendiouma@yahoo.fr)

Abstract- IP technology (Internet Protocol) formerly used only as part of the Internet, is today the carrier for many other applications such as the superior search. This use of the standard has led to a desire to pool in the heart of the network. Today, the Multi-Protocol Label Switching (MPLS) protocol of the OSI data link layer is one solution among those proposed by the IETF (Internet Engineering Task Force) to improve IP routing. The MPLS had initially intended to improve the IP routing is much used for services can offer: Quality of Service, Traffic Engineering and Virtual Private Network. The motivation in this work is two-fold: supply of our universities by cells and the study of the possibilities of interconnection of our higher schools. We propose the addition of technology VPLS.

However, to ensure the continuous supply of this VPLS IP/MPLS network, it is necessary to move towards the photovoltaic way to compensate for possible power cuts operator of the electricity grid.

Keywords: Excitons, Semiconductors, Recombination velocity, Network, Interconnexion, Router

I. INTRODUCTION

The economic growth, the development of information and communication technologies and the demand for universal access mean that the energy requirements are increasing. However, to counter any imbalances between supply and demand energetic, it is important to move towards the photovoltaic track. It is an alternative. It has been the subject of numerous studies both theoretically and experimentally. But it is only recently that the authors [2] investigated the effects of excitons on the performance of semiconductors.

However most of the work is limited to analytical processing almost neutral zone in the region p assuming dissociation and recombination of excitons are uniform in the volume of this region. In these models, the effects of coupling between electrons and excitons are considered to be neglected and phenomenological coefficients taken constant.

In this study, the author analyzes theoretically and numerically the influence of the level of excitons on the

performance of the semiconductor in the light of the space charge layer, the non-uniformity of the dissociation. It also takes into account the recombination of excitons in this area as well as the variability of the coefficients as a function of temperature. The main purpose of this study is to supply a VPLS IP/MPLS network.

The arrival of the MPLS and its evolution from communication protocols allowed to bring the simplicity of switching in networks and also to propose new technologies such as Quality of Service, traffic engineering and virtual private networks.

Therefore to actively participate in the development of our country, it is necessary to have a deployment of new infrastructure interconnecting all of our high schools to improve teaching quality and superior research. We have focused our choice on the MPLS in order to have a level of 2 VPN service based on VPLS Ethernet service that provides multipoint-to-multipoint.

In these types of networks, one uses equipment Cisco which we will have to configure in our various architectures.

The main issue will be the management needs of increasingly greater bandwidth, quality of service and electricity needs.

As network complexity is increasing and that they need the energy to form a single unit circle; numerical modeling of excitons in a semiconductor for the power supply of our university sites becomes paramount.

II. THEORY OF EXCITON

In exciton is a quasi-particle noncharged formed with a electron-hole pair associated by a coulomb interaction. This strongly related electron-hole pair is created by the absorption of photons. When the energy gap of the absorption in the material is lower where equalizes with that of the photon, there creating pair electron-hole. Furthermore relaxations photons due to excitation of the non-stop material, cause a lowering of the energy level of the electron-hole pair.

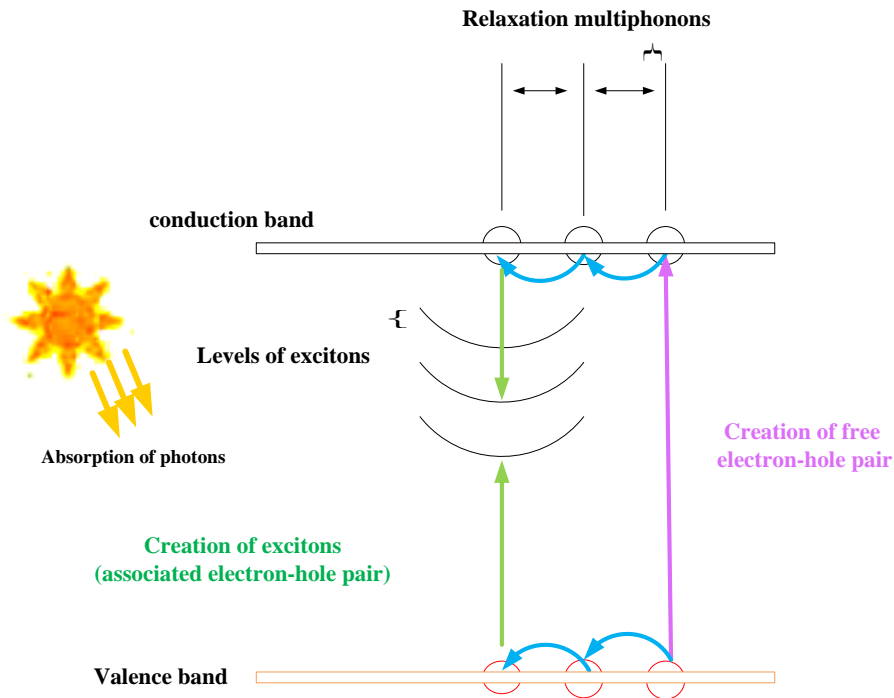


Figure 1. Procedure of creation associated electron-hole pairs (excitons) [10]

Indeed excitons are mobile, electrically neutral and highly localized. Their participation in the photocurrent in the material, results from the difference between the number of generations of pairs electron-hole and the number of recombinations. This difference increases with increasing temperature. Moreover, they are often photogenerated in semiconductors.

III. MATHEMATICAL FORMULATION AND NUMERICAL PROCEDURE

A. Mathematical formulation

We will consider a semiconductor of length L , one-dimensional character, the regions not-homogeneous doping. They are conductive. The electric field in the space charge layer is not negligible. We recognize that this electric field in the space charge layer is a linear function of the abscissa z that can be expressed in the form

$$E(z) = \frac{E_m}{w}(w - z) \text{ and } b(z) = b[E(z)] \text{ in } (0 \leq z \leq w)$$

In addition we assume that the faces $z = 0$ and $z = L$ are the site of recombination events in volume and surface.

To model the complex and tightly coupled transfers that govern the operation of the photovoltaic cell, we have established the transport equations of electrons and excitons based on certain simplifying assumptions above considered reasonable. These equations are not only coupled but contain phenomenological coefficients that depend on the temperature

field which knowledge requires the solution of equation (2) of thermal diffusion

$$F_{e0} \frac{\partial}{\partial z^*} \left\{ D_r^* \frac{\partial n_e^*}{\partial z^*} \right\} + A \frac{\partial}{\partial z^*} \{ n_e^* (w^* - z^*) \} = \frac{n_e^* n_h^* - n_{in}^{*2}}{n_e^* + n_h^* + 2n_{in}^*} + B_e (n_e^* n_h^* - n_x^* n_1^*) - C_e f_e G^* \quad (1a)$$

$$F_{x0} \frac{\partial}{\partial z^*} \left\{ R_\mu D_r^* \frac{\partial n_x^*}{\partial z^*} \right\} = (n_x^* - n_{x0}^*) - B_x (n_e^* n_h^* - n_x^* n_1^*) - C_x (1 - f_e) G^* \quad (1b)$$

$$\frac{\partial T^*}{\partial z^*} = \frac{\partial^2 T^*}{\partial z^{*2}} \quad (2)$$

With

$$z^* = \frac{z}{L}, \quad z^* = \frac{w}{L}, \quad n_e^* = \frac{n_e}{C_r}, \quad n_h^* = \frac{n_h}{C_r}, \quad n_x^* = \frac{n_x}{C_r}, \quad n_{in}^* = \frac{n_{in}}{C_r},$$

$$G^* = \frac{G_{eh}}{G_r}, \quad G^* = \frac{G_x}{G_r}, \quad t^* = \frac{a}{L^2} t, \quad T^* = \frac{T - T_a}{\Delta T_r}, \quad \Delta T_r = \frac{q_m L}{\lambda}$$

The amount D^0 is the electron diffusion coefficient calculated from the ambient temperature T_a considered constant. The "diffusion coefficient" dimensionless D_r^* expressed as:

$$D_r^* = 1 + \frac{\Delta T_r^*}{T_a} T^* \quad (3)$$

It is therefore a function of the dimensionless temperature T^* . The amount $\frac{\Delta T^*}{T_a}$ is called heat factor. Equations (1)

and (2) are closed by the initial conditions and limits dimensionless below

For the electrons

$$\begin{cases} z^* = 0 \Rightarrow n_e^*(0) = N_D^* \\ z^* = 1 \Rightarrow A_{L_e} \frac{\partial}{\partial z^*} \{D_T^* n_e^*\}_{z=1} = -[n_e^*(1) - n_{e0}^*] + B_{L_e} [n_x^*(1) - n_{x1}^*] \end{cases} \quad (4a)$$

For the excitons

$$\begin{cases} z^* = 0 \Rightarrow A_{0x} \frac{\partial}{\partial z^*} \{R_\mu D_T^* n_x^*\}_{z=0} = [n_x^*(0) - n_{x0}^*] - B_{0x} [n_x^*(0) - n_{x1}^*] \\ z^* = 1 \Rightarrow A_{L_x} \frac{\partial}{\partial z^*} \{R_\mu D_T^* n_x^*\}_{z=1} = -[n_x^*(1) - n_{x0}^*] - B_{L_x} [n_x^*(1) - n_{x1}^*] \end{cases} \quad (4b)$$

For the temperature

$$\begin{cases} t^* = 0 \Rightarrow T^*(z^*, 0) = 0 \\ z^* = 0 \Rightarrow \frac{\partial T^*}{\partial z^*} = -g(t^*) \\ z^* = 1 \Rightarrow \frac{\partial T^*}{\partial z^*} = 0 \end{cases} \quad (4c)$$

B. Numerical procedure

To solve the strongly coupled adimensional equations reduced scale obtained, we chose a numerical method. The spatial discretization with variable and tight at the interfaces of different areas of the field because of the strong gradients in these regions is adopted. The equations are then integrated into the numerical domain using the finite volume method and the coefficients are approximated by the power law Patankar scheme.

The resulting system of algebraic equations is solved by the method of double course combined with an iterative relaxation line by line type Gauss-Seidel. A study of the stability to be led to estimates of no space and time.

IV. NOMENCLATURE

Latin Letters:

a	thermal diffusivity [$\text{cm}^2 \text{s}^{-1}$]
C	Density equivalent status [m^{-3} or cm^{-3}]
D	diffusion coefficient [$\text{cm}^2 \text{s}^{-1}$]
E	Electric field [V m^{-1}]
Fact_ch	Factor heated
Fo	Relationship between time diffusion and convection
G	generation rate [$\text{N cm}^{-3} \text{s}^{-1}$]
K	Boltzmann constant [JK^{-1}]
L	The diffusion length [cm]
n	Concentration of carriers, [m^{-3} or cm^{-3}]
q	Electric charge [C]
R	Rate of exciton recombination of electrons [$\text{cm}^{-3} \text{s}^{-1}$]
S	Recombination velocity [cm s^{-1}]
t	time [s]

T	Temperature dimensional [K]
U	recombination rate [$\text{cm}^{-3} \text{s}^{-1}$]
W	width of the depletion zone [cm]

Greek symbols:

α	absorption coefficient [μm^{-1}]
λ	wavelength of the light source [μm]
μ	mobility of electrons and excitons [$\text{cm}^2 \text{v}^{-1} \text{s}^{-1}$]
ρ	Average density of the semiconductor, [kg m^{-3}]
τ	lifetime of electrons and excitons [s]

Indices Exhibitor:

A	acceptor
D	donor
e	on the electron
x	relative to the exciton
h	relative to the hole
in	intrinsic
m	average
o	at equilibrium
i	th component
(*)	Related to the dimensionless variables
(°)	Relative to a constant

V. PHOTOCURRENT DENSITY OF CHARGE CARRIERS: WITH A VOLUME OF COUPLING COEFFICIENT $bv\{E(z)\}$

The volume coupling coefficient $bv\{E(z)\}$ and the total photocurrent density of electrons and excitons have been developed in [2] and [6].

The analysis of a curve in the other (Figures 2) shows that the total photocurrent density is due to the excitons as photocurrent density of electrons decreases according to the recombination velocity. These results show the effect of excitons on the total density of photocurrent.

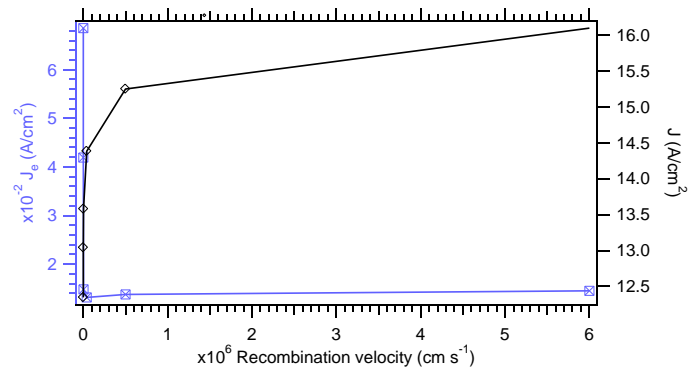


Figure 2. Photocurrent density of charge carriers as a function of the recombination velocity for a silicon-based solar cell. $N_A=10^{16} \text{ cm}^{-3}$; $N_D=10^{19} \text{ cm}^{-3}$; $n_i=1.45 \cdot 10^{10} \text{ cm}^{-3}$; $n_{\text{mott}}=1.0310^{18} \text{ cm}^{-3}$; $Fo=10$; $\text{Fact_ch}=2 \cdot 10^{-2}$; $bv_{\text{inf}}=10^{-16} \text{ cm}^3 \text{ s}^{-1}$; $bv_{\text{max}}=10^{-7} \text{ cm}^3 \text{ s}^{-1}$; $bs_{\text{max}}=10^{+1} \text{ cm s}^{-1}$; $L_e \neq L_x = f$ (average temperature)

A. Influence of volume coupling coefficient

Figure 3 reproduced the total density of photocurrent of the charge carriers according to the recombination velocity for low the, average ones and strong values of the volume coupling coefficient.

From one curve to another on figure 3, an analysis of the variation of the total density of photocurrent according to the recombination velocity shows a total packing of photocurrent for the strong couplings and a reduction for the weak ones and average voluminal couplings. For speeds of higher or equal recombinations $0,5 \text{ cm s}^{-1}$, the total density of photocurrent are almost constant but, for the weak ones and average voluminal couplings, few carriers cross the junction.

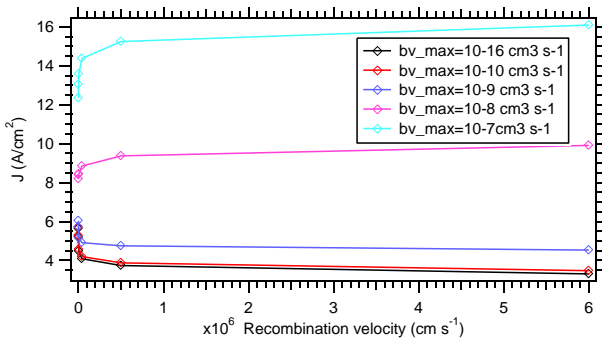


Figure 3. Influence of volume coupling coefficient to the variation of the total density of photocurrent of the charge carriers depending on the recombination velocity. $N_A=10^{16} \text{ cm}^{-3}$; $N_D=10^{19} \text{ cm}^{-3}$; $n_i=1.45 \cdot 10^{10} \text{ cm}^{-3}$; $n_{\text{mott}}=1.0310^{18} \text{ cm}^{-3}$; $b_s=10^{+1} \text{ cm s}^{-1}$; $F_0=10$; $\alpha(\lambda)=0$; $f_x=1$; $f_e=0$; $\text{Fact}_{\text{ch}}=2 \cdot 10^{-2}$; $bv_{\text{inf}}=10^{-16} \text{ cm}^3 \text{ s}^{-1}$; $L_e \neq L_x=f$ (average temperature)

B. Influence of conversion velocity

Variation of the total density of photocurrent, according to the recombination velocity reproduced on figure 5 fact of appearing an increase in this last for the weak ones and average values the conversion velocity. Whereas, for the strong values the conversion velocity we have two stages: the first stage corresponds to a reduction in the total density of photocurrent and the second with his increase. Reduction in the total density of photocurrent for the low values the recombination velocity, with $b_s = 10^{+7} \text{ cm s}^{-1}$ is explained by the diffusion of the charge carriers towards the base. It is much easier for the latter to diffuse towards the interfaces and to recombine there to be collected by the junction.

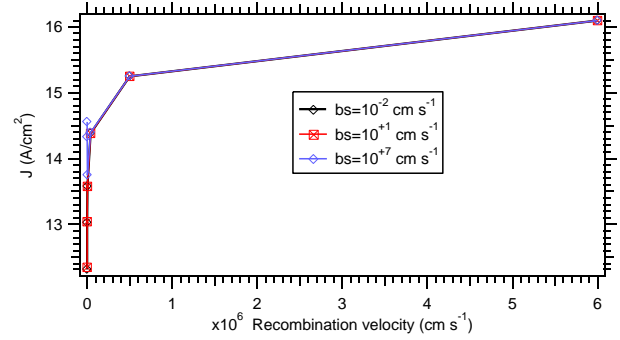


Figure 4. Influence of conversion velocity to the variation of the total density of photocurrent of the charge carriers depending on the recombination velocity. $N_A=10^{16} \text{ cm}^{-3}$; $N_D=10^{19} \text{ cm}^{-3}$; $n_i=1.45 \cdot 10^{10} \text{ cm}^{-3}$; $n_{\text{mott}}=1.0310^{18} \text{ cm}^{-3}$; $\alpha(\lambda)=0$; $f_x=1$; $f_e=0$; $\text{Fact}_{\text{ch}}=2 \cdot 10^{-2}$; $F_0=10$; $bv_{\text{inf}}=10^{-16} \text{ cm}^3 \text{ s}^{-1}$; $bv_{\text{max}}=10^{+7} \text{ cm}^3 \text{ s}^{-1}$; $L_e \neq L_x=f$ (average temperature)

C. Influence factor of heating on total density of photocurrent

We represent on figure 5 the total density of photocurrent depending on the recombination velocity for various values of the factor of heating. Increase in this last A a considerable effect on the variation of the total density of photocurrent. It supports the thermo generation of the charge carriers: that wants to say that with a high factor of heating the phenomenon of thermo generation prevails on that of recombination.

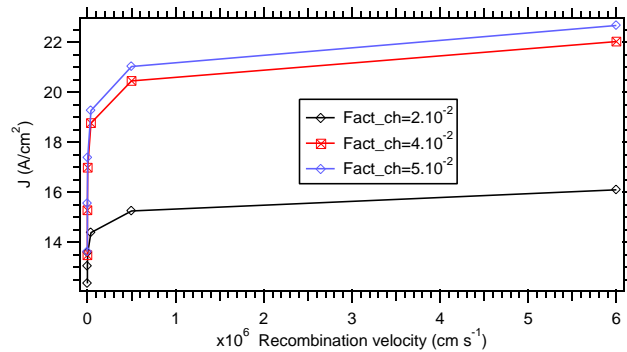


Figure 5. Influence of heating factor to the variation of the total density of photocurrent of the charge carriers depending on the recombination velocity. $N_A=10^{16} \text{ cm}^{-3}$; $N_D=10^{19} \text{ cm}^{-3}$; $n_i=1.45 \cdot 10^{10} \text{ cm}^{-3}$; $n_{\text{mott}}=1.0310^{18} \text{ cm}^{-3}$; $\alpha(\lambda)=0$; $f_x=1$; $f_e=0$; $F_0=10$; $bv_{\text{max}}=10^{+7} \text{ cm}^3 \text{ s}^{-1}$ et $bv_{\text{max}}=10^{+1} \text{ cm}^3 \text{ s}^{-1}$; $bv_{\text{inf}}=10^{-16} \text{ cm}^3 \text{ s}^{-1}$; $L_e \neq L_x=f$ (average temperature)

In short, analysis of the variation of the total density of photocurrent according to the recombination velocity for $bv=b\{E(z)\}$; show that we have almost perfect interfaces with: voluminal couplings, a factor of heating and a number of Fourier high. Whereas at the low of recombination velocities, one needs small values the conversion velocity.

We have just determined the parameters physical, kinematics and intrinsic most significant for the operation of our system photovoltaic. Now, we will try to make the audit of the telecommunications network which we will connect on the electrical supply network of solar cells containing silicon. Each one of these cells, is subjected to a monochromatic illumination by the front face and to a heat insulation by the back face [5]. In addition, we will test virtualiser our network VPLS IP/MPLS by using software GNS3.

VI. SIMULATION

The objectives of the simulation are:

- To ensure the connectivity of researchers from the University Cheikh Anta Diop with those of University Gaston Berger in St. Louis (SENEGAL) ;
- To minimize the number of lost packets at the access routers (LER) of the MPLS backbone.

Then we can assume that: the simulation focuses on the loss at the MPLS nodes; all links are full-duplex type and each source is able to transmit and receive simultaneously.

A. Addressing plan

There are several possibilities for addressing plan. The choice should be based on current and future needs.

The use of private addressing is justified for the following reasons:

- The introduction of a simple and effective security policy;
- The independence of the availability or unavailability of a new official class C for an extension of the network;
- The visibility of the network, in the case of connections at the ends, it will be easy to spot the stream carrying the intranet clients.

For addressing Sites (LAN and equipment), one approach would be to use class A 10.0.0.0 255.255.255.0 with mask.

- 10.0.0.2/32 - router PE UGB
- 10.0.1.0/24 - Subnet 1
- 10.0.2.0/24 - Subnet 2
- 10.0.3.0/24 - Subnet 3
- 10.0.4.0/24 - Subnet 4
- 10.0.5.0/24 - Subnet 5
- 10.0.6.0/24 - Subnet 6
- 10.0.7.0/24 - Subnet 7

This choice is made based on the current and future needs on one hand and the other based on the establishment of a simple and effective security policy. It is also based on the independence of the availability or unavailability of a new official class C for a network extension to other Universities and visibility of the network, in the case of connections at the ends.

Network powered by the system photovoltaic

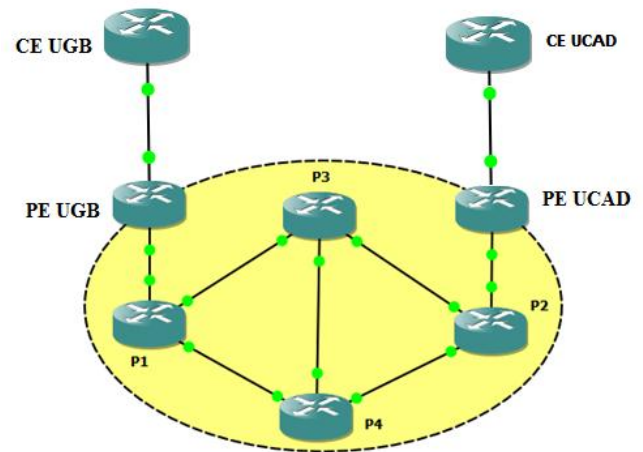


Figure 6. Interconnection between the CE and PE of attachment

B. Configuring PE UCAD and UGB (VPLS)

Here it is first interconnection between PE

In this section, our goal is to verify connectivity between University Gaston Berger (UGB) and University Cheikh Anta Diop (UCAD) in Dakar. Therefore, the labels used by PE UGB to join all loopback addresses MPLS network routers are our starting point. Loopback addresses are the addresses of local routers interfaces. In this particular configuration, if the primary interface goes, there is another way. Moreover, as MPLS OSPF runs on the router advertises this IP address into OSPF for the sake of fault tolerance.

C. Configuration MPLS VPN

We are interested in that part of the deployment of a virtual private network VPN routing packets through the interconnection between the CE and PE

We start by building a VRF table, running OSPF in the VRF instance and run MP-BGP for the announcement of the roads.

D. The routing of packets

To understand how to pass the packets and what labels are affixed by MPLS and learn the status of the message, one must make a ping or traceroute from a router CE UGB (VPN GREEN) to the router CE UCAD. Therefore it is viewed from the router CE UGB (VPN GREEN) to perform these two commands.

Here's the result:

```

PE UGB
Router#traceroute vrf GREEN 200,200,0,2
Type escape sequence to abort.
Tracing the route to 200,200,0,2
 0 10.0.1.2 [MPLS: Labels 17/19 Exp 0] 16 msec 16 msec 36 msec
 1 200,200,2,254 [MPLS: Label 19 Exp 0] 36 msec 12 msec 32 msec
 2 200,200,2,1 60 msec 44 msec *
Router#

```

We find that the package leaves the router PE UGB to the router P1 with two labels. They are labels 17 and 19. The label 17 is used to switch the packet in the backbone. P1 router is therefore in its commutation table and seeks the output interface and output label corresponding to an input label 17. The output interface is the interface to the router PE UCAD; no output label. P1 router so removes the label 17, which is intuitive because the package is now coming to a PE UCAD. That is why in the second line of the screenshot there is more than a label.

The router PE UCAD looks in its commutation table and finds the interface and the corresponding output label. It removes the label 19 and transmits the packet to the router CE UCAD. This is why, in the last line of traceroute there is no label.

VII. TERMINOLOGY	
BGP	Border Gateway Protocol
CE	Custom Edge router
ECMP	Equal Cost Multi Path
FEC	Forwarding Equivalence Class
IP	Internet Protocol
IGP	Interior Gateway Protocol
IETF	Internet Engineering Task Force
LAN	Local Area Network
LDP	Label Distribution Protocol
LER	Label Edge Router
LSR	Label Switching Router
MGW	Media Gateway
MP-BGP	Multi Protocol Border Gateway Protocol
MPLS	Multiprotocol Label Switching
OSPF	Open Shortest Path First
P	Provider
PE	Provider Edge router
VPLS	Virtual Private LAN Service
VPN	Virtual Private Network
VRF	Virtual Routing and Forwarding

VIII. CONCLUSION

The numerical study of the influence of the level of excitons in the semiconductor for feeding a VPLS IP/MPLS network is made with a volume coupling coefficient which depends on the exciton dissociation field and temperature average. The finite volume method was used to discretize the equations of transport of the charge carriers in permanent regime and the heat. These equations are solved by using Thomas algorithm.

It comes out from our study that the total density of photocurrent depending on the recombination velocity is due to excitons. It as comes out from our work as the total density of photocurrent obtained for fixed physical parameters is high enough for a solar cell in a photovoltaic site of system. For such parameters we have: the volume coupling coefficient, the conversion velocity of excitons in free electrons and the factor of heating.

Our work by simulating a GNS3 network simulator was completed. The CE does not know the switch; they are routing using OSPF protocol type. Once in the backbone by cons, the packets are switched by means of MPLS. In terms of security, a packet cannot be routed to that one site to another. It is impossible for a package came from the outside to be routed to a site; conversely a packet from a VPN site can move that to another VPN site. A special feature of this solution is that several VPNs can run in parallel, without having any idea of each other's presence.

This study is still open to further improvements. It deserves to be thorough and complete. A logical extension of this work would be to interconnect all the schools and universities of Senegal or Africa by making a design of solar cells and VPLS IP/MPLS network.

APPENDIX	
$F_{0e} = \frac{\tau_e D^0}{L^2}$	$F_{0x} = R_\mu \frac{\tau_x D^0}{L^2}$
$A = \frac{\mu_e \tau_e E_m}{w}$	$A_{eL} = \frac{D^0}{LS_e}$
	$A_{xL} = \frac{D^0}{LS_x}$
	$A_{0x} = \frac{D^0}{LS_{0x}}$
$B_{eL} = \frac{b_s}{S_e}$	$B_{xL} = \frac{b_s}{S_x}$
	$B_{0x} = \frac{b_s}{S_{0x}}$
$B_e = \tau_e b C_r$	$B_x = \tau_x b C_r$
$C_e = \frac{\tau_e G_r}{C_r}$	$C_x = \frac{\tau_x G_r}{C_r}$
$G_{eh} = G_{eho} \exp(-\alpha z)$	$G_x = G_{xo} \exp(-\alpha z)$
$G_{eho} = f_e \alpha(\lambda) N(\lambda)$	$G_{xo} = f_x \alpha(\lambda) N(\lambda)$
$N(\lambda) = 5.03110^{+18} \lambda P(\lambda)$	
$\alpha(\lambda) = 0.526367 - 1.14425/\lambda + 0.585368/\lambda^2 + 0.039958/\lambda^3$	

REFERENCES

- [1] D. E. Kane, R. M. Swanson: The effects of excitons on apparent band gap narrowing and transport in semiconductors, J. Appl. Phys. 73, 1193-1197 (1993).
- [2] M. Burgelman, B. Minnaert ; Including excitons in semiconductor solar cell modeling. Thin Solid Films 511-512, 214-218 (2006).
- [3] S. Zh. Karazhanov ; Temperature and doping level dependence solar cell performance Including excitons. Solar Energy Materials & Solar Cells 63 (2000) 149-163.
- [4] R. Corkish, D. S. P. Chan, and M. A. Green ; Excitons in silicon diodes and solar cells: A three-particle theory. Institute of Physics. [(S0021 - 8979 (1996) 0070 - 9)].
- [5] M. Faye, M. MBow, M. Ba: Numerical Modeling of the Effects of Excitons in a Solar Cell Junction n-p of the Model by Extending the Space Charge Layer, International Review of Physics (I.RE.PHY), Vol. 8, N. 4 ISSN 1971-680X (August 2014).
- [6] M. Faye, M. MBow, M. Ba: Development a Numerical Model Applicable to Inorganic and Organic Solar Cells Based on Silicon in the Presence of Excitons, Current Trends in Technology and Science, ISSN: 2279-0535. Volume: 04, Issue: 02 (Feb - Mar. 2015)

- [7] Y.Zhang, A.Mascarenhas, S. Deb: Effets of excitons in solar cells J. Appl. Phys. 84 3966-3971 3966 (1998).
- [8] S.V.Patankar: "Numerical Heat Transfer and Fluid Flow", Hemisphere Publishing Corporation, McGraw-Hill Book Company, 1981.
- [9] R. B. BIRD, W. E. STEWART, E N. LIGHTFOOT: Transport Phenomena, John Wiley and Sons, Inc, New York 2001.
- [10] Laurent Badie, Etude de matériaux amplificateurs à base de nanoparticules et réalisation d'un composant polymère pour les télécommunications optiques, Thèse de Doctorat, Ecole normale supérieure de Cachan, 19 Décembre 2008.
- [11] David TORTEL, Anne CHEVALIER, Louis DE TERSANT, Initiation à MPLS, MPLS VPN, 7 juillet 2009
- [12] Paul Brittain, Adrian Farrel: "A review of the implementation options for MPLS VPNs including the ongoing standardization work in the IETF MPLS Working Group" Metaswitch Networks, First issued November 2000.